

Mechanical characterization of melt-textured $Y_{0.95}Er_{0.05}Ba_2Cu_3O_{7-\delta}$ superconductor prepared in air

Lincoln Brum de Leite Gusmão Pinheiro^a, Alcione Roberto Jurelo^{a,*}, Francisco Carlos Serbena^a, Pedro Rodrigues Jr.^a, Carlos Eugênio Foerster^a, Adilson Luiz Chinelatto^b

^a Departamento de Física, Universidade Estadual de Ponta Grossa, Av. Gen. Carlos Cavalcanti No. 4748, 84030-000 Ponta Grossa, Paraná, Brazil

^b Departamento de Engenharia de Materiais, Universidade Estadual de Ponta Grossa, Av. Gen. Carlos Cavalcanti No. 4748, 84030-000 Ponta Grossa, Paraná, Brazil

ARTICLE INFO

Article history:

Received 23 December 2009

Received in revised form 11 February 2010

Accepted 25 March 2010

Available online 1 April 2010

Keywords:

High- T_C superconductor

Hardness

Elastic modulus

Instrumented indentation

Vickers indentation

ABSTRACT

The effect of Er substitution on the mechanical properties of *ab*- and *a(b)c*-planes of melt-textured $YBa_2Cu_3O_{7-\delta}$ is reported in the present work. The non-oxygenated samples were characterized by scanning electron microscopy, X-ray diffraction and mechanical properties by instrumented indentation and conventional Vickers indentation whereas the superconducting properties were determined by resistivity measurements on oxygenated samples. The X-ray pattern and EDS analysis revealed the presence of Y-123, Y-211 and $BaCeO_3$ phases. Er substitution up to 5 wt.% did not affect the superconducting properties. No difference in hardness was observed for the *ab*- and *a(b)c*-planes. Elastic modulus of the *a(b)c*-plane was 10% higher than of the *ab*-plane. Differences in indentation fracture toughness obtained by conventional Vickers indentation of the *ab*- and *a(b)c*-planes was observed. The addition of 5 wt.% of Er did not affect significantly the mechanical properties of melt-textured samples when compared with pure melt-textured $YBa_2Cu_3O_{7-\delta}$.

© 2010 Elsevier B.V. All rights reserved.

1. Introduction

High- T_C superconductors are important in transport processes like supporting high critical current density and trapping of high magnetic fields. In addition to its electrical and magnetic properties, they must also have good mechanical performance for actual technological bulk applications.

Er has been added with the aim to produce larger melt-textured samples. Up to now, there is little knowledge about its effect on the mechanical properties of Er substitution into melt-textured-growth $YBa_2Cu_3O_{7-\delta}$ (YBCO). For example, from tensile tests of $YBa_2Cu_3O_{7-\delta}$ blocks welded by $ErBa_2Cu_3O_{7-\delta}$ superconducting solder at room temperature, it was observed that the tensile strength $YBa_2Cu_3O_{7-\delta}/ErBa_2Cu_3O_{7-\delta}$ joint was smaller than $ErBa_2Cu_3O_{7-\delta}$ bulk [1]. Moreover, Iida et al. [2] showed that two melt-textured $YBa_2Cu_3O_{7-\delta}$ superconductor blocks were successfully welded with $ErBa_2Cu_3O_{7-\delta}$ solder having a lower peritectic temperature than that of $YBa_2Cu_3O_{7-\delta}$.

It was also observed that some of the $REBa_2Cu_3O_{7-\delta}$ compounds (such as for RE = Nd, Sm, Gd, Ho and Er) exhibit antiferromagnetic ordering below T_C [3] showing that the investigation about the interplay between superconductivity and magnetism can be of particular interest in this system. For example, Ivanshin et al. [4,5]

found existence of the peculiarities of magnetic interactions between Er^{3+} and Cu^{2+} showing that this has an effect on the superconducting CuO_2 planes and consequently on the pinning energy of vortices.

Studies devoted to the effect of Er substitution on the physical properties of YBCO pellets have shown its numerous advantages. However, the aim of this study is to produce and characterize single domain melt-textured $Y_{0.95}Er_{0.05}Ba_2Cu_3O_{7-\delta}$ superconductor pellets. For that, samples were characterized by scanning electron microscopy and microprobe energy dispersive spectroscopy (EDS), X-ray diffraction and electrical resistivity measurements. The study of mechanical properties, hardness (H) and elastic modulus (E), were measured by instrumented indentation on *ab*- and *a(b)c*-planes. The indentation fracture toughness (K_C) was evaluated for both planes after conventional Vickers indentation.

2. Experimental details

$Y_{0.95}Er_{0.05}Ba_2Cu_3O_{7-\delta}$ top seeding growth samples were prepared to obtain single domain. A sintered ceramic pellet of $Y_{0.95}Er_{0.05}Ba_2Cu_3O_{7-\delta}$ (Y-123) was prepared at 920 °C for 24 h. After that, a $NdBa_2Cu_3O_{7-\delta}$ single crystal seed was placed on top of the sample and the whole system was heated above 1040 °C (the peritectic temperature). Finally, the sample was drawn during cooling to an undercooled state from 1020 °C to 990 °C at a cooling rate of 10 °C/h to induce crystallization. The final composition of

* Corresponding author. Tel.: +55 42 220 3044; fax: +55 42 220 3042.
E-mail address: arjurelo@uepg.br (A.R. Jurelo).

the sintered ceramic was typically (70 wt.% $Y_{0.95}Er_{0.05}Ba_2Cu_3O_{7-\delta}$ + 30 wt.% Y_2BaCuO_5) + 1 wt.% CeO_2 . For resistivity measurements, some melt-processed samples were cut from the textured monodomain and oxygenated at 420 °C during five days under pure flowing oxygen (around 0.08 cm³/s).

The X-ray diffraction patterns were obtained from 10° to 100° in the 2θ range with 0.02° steps and counting time of 4 s for ab - and $a(b)c$ -orientations of bulk samples. The measurements were performed using a Shimadzu X-ray diffractometer with Cu K_α radiation and the crystal structure and composition analyses were performed using the GSAS program [6] with the EXPGUI interface [7]. The electrical resistivity as a function of temperature was measured by means of a four-probe AC technique at the frequency of 37 Hz. The temperature was determined with an accuracy of 0.01 K by precisely measuring the resistance of a Pt-100 sensor. Hardness and elastic modulus profiles were determined by using an instrumented indenter (Nanoindenter XP) with diamond Berkovich tip and following the Oliver & Pharr method [8]. The applied loads were in the range from 1.6 to 400 mN in a 5×4 indentation matrix for each plane. The distance between each indentation was 50 μ m. Care was taken to perform the indentations in a region free of pores and cracks. Vickers indentations at 10 N were employed to measure hardness and indentation fracture toughness on ac - and $a(b)c$ -planes using a Shimadzu HMV-2T microindenter. The tests were performed at room temperature in air with 50–80% relative humidity. Indentation fracture toughness was calculated according to the relation proposed by Anstis et al. [9]:

$$K_C = \alpha \cdot \sqrt{\frac{E}{H_V}} \frac{P}{c^{3/2}} \quad (1)$$

where α is a constant equals to 0.016 ± 0.04 , H_V is the Vickers hardness, c is the radial crack length emanating from the Vickers indentation and P is the applied load. The microstructure was revealed by thermal etching at 850 °C for a few seconds followed by fast cooling. This thermal treatment did not produce grain growth. Samples surface morphology and indentation impressions were observed by scanning electron microscopy (SEM).

3. Results and discussion

Fig. 1 shows the X-ray diffraction pattern for the $a(b)c$ -plane. The X-ray pattern reveals the presence of the Y-211, Y-123 and $BaCeO_3$ phases. EDS analysis confirmed the presence of $BaCeO_3$ inclusions, dispersed in the $(Y_{0.95}Er_{0.05})Ba_2Cu_3O_{7-\delta}$ matrix. We assumed

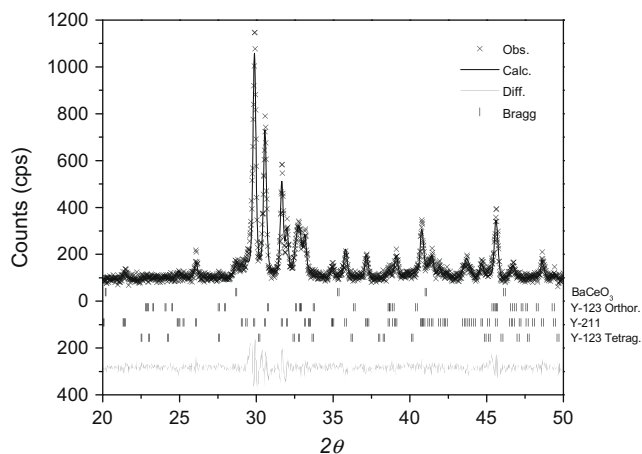


Fig. 1. Experimental, calculated and difference profiles of the X-ray diffraction pattern for $a(b)c$ -plane of melt-textured $Y_{0.95}Er_{0.05}Ba_2Cu_3O_{7-\delta}$ sample.

that the matrix is composed of both tetragonal and orthorhombic phases because samples presented high resistivity at room temperature, which can be due to poor oxygenation of the orthorhombic phase or to the presence of the tetragonal phase [10].

Rietveld refinement of the diffraction pattern was performed assuming the presence of the orthorhombic and tetragonal phases of $(Y_{0.95}Er_{0.05})Ba_2Cu_3O_{7-\delta}$, the Y-211 and the $BaCeO_3$ phases. The unit cell parameters and the volume for each phase are shown in Table 1 from refinement of the $a(b)c$ -plane. The lattice parameters and calculated unit cell volumes are in agreement with literature data [10]. The R_p (R -pattern), R_{wp} (R -weighted pattern) and χ^2 (goodness-of-fit) were 0.13, 0.14 and 2.5, respectively. These values are compatible with the low count statistics of the measured profile.

Fig. 2a and b show SEM micrographs for ab - and $a(b)c$ -planes of $Y_{0.95}Er_{0.05}Ba_2Cu_3O_{7-\delta}$. Preferred orientation for grain growth is known to be in the ab -plane and thus grains are expected to be aligned along this direction. In the figures are indicated Y-211

Table 1

Lattice parameters a , b , c and V (unit cell volume) for $Y_{0.95}Er_{0.05}Ba_2Cu_3O_{7-\delta}$, $Y_{0.95}Er_{0.05}Ba_2Cu_3O_6$, Y_2BaCuO_5 and $BaCeO_3$ obtained from Rietveld refinement.

Phase	a (Å)	b (Å)	c (Å)	V (Å ³)
$Y_{0.95}Er_{0.05}Ba_2Cu_3O_{7-\delta}$	3.820 (3)	3.897 (2)	11.64 (1)	173.3 (2)
Y_2BaCuO_5	7.1272 (4)	12.1740 (4)	5.6554 (3)	490.71 (5)
$BaCeO_3$	4.400 (2)	4.400 (2)	4.400 (2)	85.2 (1)
$Y_{0.95}Er_{0.05}Ba_2Cu_3O_6$	3.864 (2)	3.864 (2)	11.84 (3)	176.9 (5)

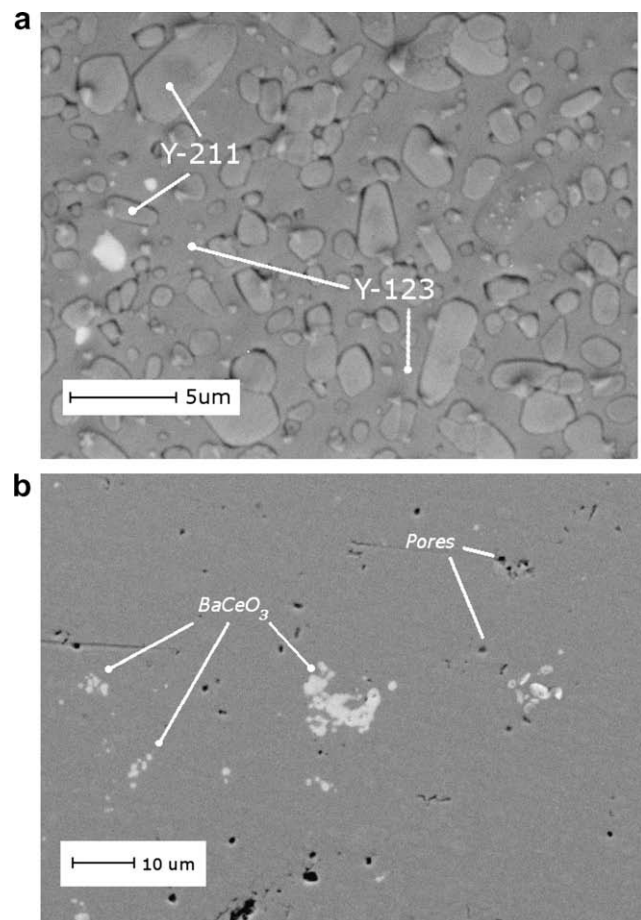


Fig. 2. SEM micrographs of: (a) thermal etched ab - and (b) $a(b)c$ -planes of $Y_{0.95}Er_{0.05}Ba_2Cu_3O_{7-\delta}$ sample.

Download English Version:

<https://daneshyari.com/en/article/1818772>

Download Persian Version:

<https://daneshyari.com/article/1818772>

[Daneshyari.com](https://daneshyari.com)